Optical and Quantum Electronics (2024) 56:1198
https://doi.org/10.1007/s11082-024-06829-2

Interference effect in surface modified ZnS nanoparticles / Poly (methylmethacrylate) nanocomposites

Nebojsa Romcevic[1] · Branka Hadzic[1] · Milica Curcic[1] · Vesna Radojevic[2] · Novica Paunovic[1] · Maja Romcevic[1]

Received: 28 September 2023 / Accepted: 11 March 2024 / Published online: 18 June 2024

Abstract
Surface modified ZnS nanoparticles / poly (methylmethacrylate) - (PMMA) nanocomposites were prepared by the solution casting method. The ZnS nanoparticles, as starting materials in the present study, were synthesized mechanochemically and their crystallite size was estimated as 2.3 nm. Surface modification of obtained nanoparticles was performed by 3-Mercaptopropyltrimethoxysilane. We investigate thin samples of the nanocomposite material and pure PMMA (about 290 μm) with a strong interference effect, and corresponding thick samples, as reference. The optical properties of this material were studied by far-infrared spectroscopy. The analysis of the far-infrared reflectivity spectra was made by the fitting procedure, according to the model for a thin plate of nanocomposites in the air. The dielectric function of the nanocomposites was modeled as a mixture of homogenous surface modified ZnS spherical inclusions in PMMA, by the Maxwell-Garnet formula. In the case of a PMMA thin sample, intense, well-defined interference was registered in the range of 90 to 200 cm^{-1}, while significantly weaker and less well-defined interference was registered in the range around 450 cm^{-1}. In the thin composite sample, in addition to the interference induced by sample thickness, interference induced by the existence of ZnS nanoparticles was also observed, located between the TO and LO phonons of ZnS. This opens the possibility of applying nanocomposites in interferometry.

Keywords Nanocomposites · Interference effect · Far-infrared spectroscopy · Effective medium theory

1 Introduction

Nanostructures in which the properties of organic molecules are combined with the optoelectronic properties of semiconductors are the best examples of theoretical and experimental research that found its place in the industry. At present, this primarily refers to the color control of these structures, as a direct consequence of quantum confinement of electronic states (Murray et al. 1993). This effect found its application in optoelectronic systems such as light-emitting diodes (Colvin et al. 1994; Dabbousi et al. 1995) and photovoltaic cells

Extended author information available on the last page of the article

(O'Regan et al. 1991), or as components of future nanoelectronic devices. The search for new nanodimensional systems and effects that can lead to their new applications is ongoing and represents a significant challenge.

One of the interesting phenomena is interference. This effect is exploited in many areas and the most important is interferometry. Interferometry has contributed to the further advancement of physics and has successfully applied in a large number of physical and engineering measurements (optical interferometry, astronomical interferometer, acoustic interferometry…) (Steel 1986).

Thin-film interference, as a narrower case of the mentioned phenomena, is an occurrence in which waves, reflected from the upper and lower border of the thin film, interfere and enhance or reduce the reflected light. In principle, which of these two phenomena will occur depends on the thickness of the thin film. But, at the same time, the thin-film interference is also a function of the type of the film or layer which means that the control of the effective refractive index of the layer can significantly affect the effect itself (Stavenga 2014). In that sense, the composite materials can play a very important role in this area since changing the composition of the thin film, for the same thickness, can lead to different interference.

Polymer nanocomposite usually consists of an organic polymer which forms a matrix in which inorganic components (semiconductors) are dispersed. One of the common matrices in polymer nanocomposites is poly (methylmethacrylate) – PMMA, due to its favorable properties such as excellent transparency and ultraviolet resistance, as well as good abrasion resistance hardness, and stiffness (Peppas et al. 1994). Matrix-nanoparticles interface has an important role in the physic-mechanical behavior of nanocomposites. Due to their extremely small sizes, nanomaterials cannot be used on a large scale, particularly as long-bearing materials in engineering applications. For this, there has long been a desire to develop bulk composites incorporating these nanomaterials to harness their extraordinary properties in bulk applicable materials. Initial ideas and principles are given in (Dzenis 2008).

In our earlier paper (Romcevic et al. 2022), surface modified ZnS nanoparticles by 3-Mercaptopropyltrimethoxysilane were synthesized and analyzed to obtain a core-shell structure.

In this work, such surface modified ZnS nanoparticles are embedded in the thin films of PMMA to obtain a new nanocomposite material with modified characteristics for the improved application of the interference phenomena.

2 Methods and materials

The sample morphology was analyzed using the high-resolution MIRA3 TESCAN scanning electron microscope (SEM) operated at the accelerating voltage of 5, 12, and 20 kV. Far-infrared reflection spectra were recorded in the wave number range up to 600 cm^{-1} utilizing an A BOMEM DA – 8 FTIR spectrometer with a deuterated triglycine sulfate (DTGS) pyroelectric detector.

The ZnS nanoparticles were synthesized by mechanochemical treatment, detailly described in the literature (Dutkova et al. 2009; Trajic et al. 2015; Trajic et al. 2016). The milling time was 10 min and the crystallite size of the obtained ZnS nanoparticles was estimated to be 2.3 nm. Surface modification of ZnS is achieved by using a 3-Mercaptopropyl-

trimethoxysilane (MPTMS) – Dynasylane, Evonik Industries, and toluene, hexane (Sigma Aldrich) as solvent (Romcevic et al. 2022; Curcic et al. 2020).

Surface modified ZnS nanoparticles / poly (methylmethacrylate) - PMMA nanocomposites were prepared by the solution casting method. The ZnS nanoparticles modified with MPTMS were added to the solution of the PMMA (concentration of 22% wt.) to achieve the nanoparticles concentration of 0.06% wt. The thin films were obtained by casting the solutions in Petri dishes and dried in the same way as the previous samples. Considering the thickness of the thin film we obtained the same types of samples: conditionally thin - about 290 μm and thick - over 2 mm.

3 Results

The micrographs of surface modified ZnS nanoparticles / PMMA nanocomposites, with different resolutions, are given in Fig. 1. The clusters of about 60 nm, are visible. Unevenness on the surface of the sample is present in the case of thin and thick samples.

The far-infrared spectra of surface modified ZnS nanoparticles / PMMA nanocomposites and pure PMMA, at room temperature, are presented in Fig. 2a (thick samples) and Fig. 2b (thin samples). Firstly, the difference in spectra of pure PMMA and surface modified ZnS nanoparticles is registered in both cases, in the ranges at about 200 cm^{-1}, 300 $cm^{-1,}$ and 450 cm^{-1}. Also, on thin samples of PMMA, with and without surface modified ZnS nanoparticles (Fig. 2b), we have the appearance of interference. This effect is not present in thick samples, as expected. Intensive, a well-defined interference is registered in the range from 90 to 200 cm^{-1}. The experimental spectrum of PMMA in this range shows 10 interference maxima ranging from 97.40 cm^{-1} to 196.57 cm^{-1}. On the other hand, the experimental spectrum of ZnS nanoparticles / PMMA nanocomposites has 9 maxima from 95.05 cm^{-1} to 194.16 cm^{-1}. Considerably weaker and poorly defined interference was registered in the range around 450 cm^{-1}, in the case of both samples. In the far-infrared spectrum for the thin sample surface modified ZnS nanoparticles / PMMA nanocomposite, in the range from 240

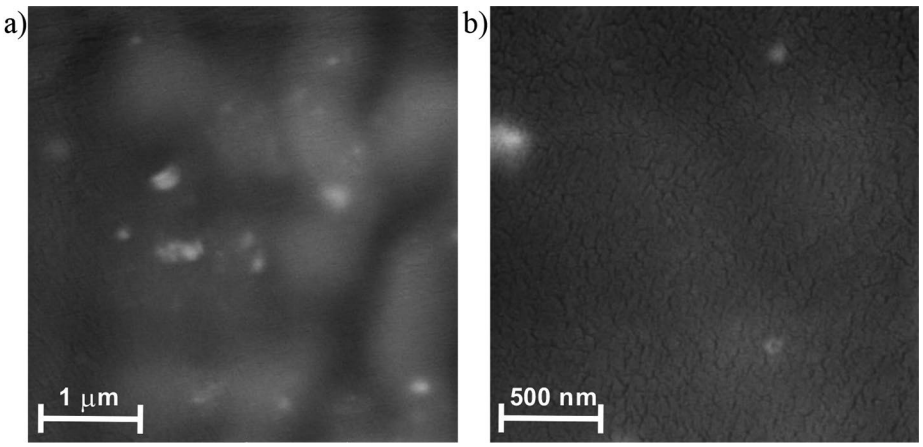

Fig. 1 SEM images of surface modified ZnS nanoparticles / PMMA nanocomposite, with different resolutions for **a**) Thick samples (2 mm) and **b**) Thin samples (290 μm)

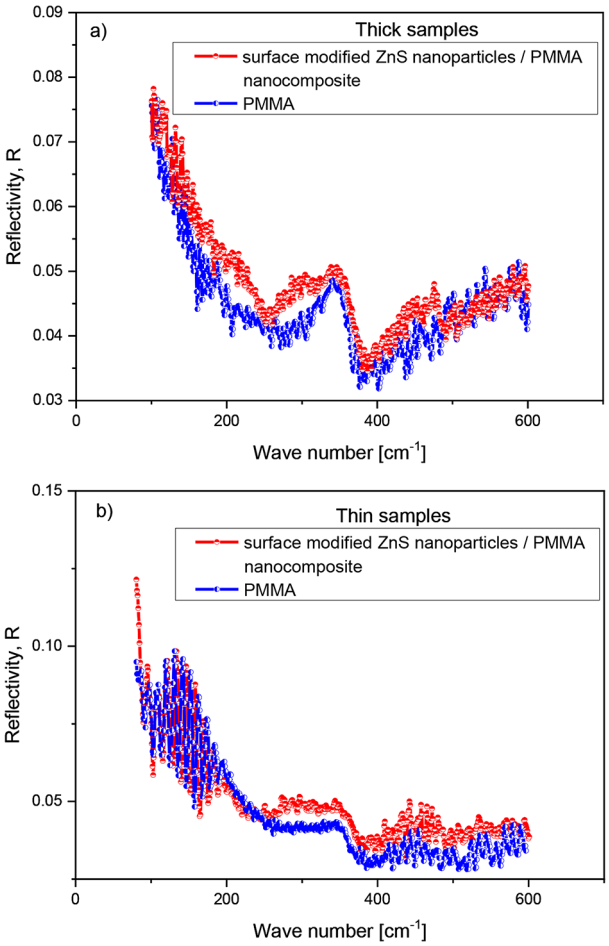

Fig. 2 Experimental far-infrared reflection spectra. **a**) Thick samples (2 mm). PMMA (blue line), surface modified ZnS nanoparticles / PMMA nanocomposite (red line). **b**) Thin samples (290 μm). PMMA (blue line), surface modified ZnS nanoparticles / PMMA nanocomposite (red line)

to 350 cm^{-1}, a very weak, poorly defined interference was detected additionally. It can be said that we have the first maximum at 243.78 cm^{-1}, and the tenth at 341.31 cm^{-1}.

4 Discussion

The analysis of the far-infrared reflectivity spectra, as we'll see, was made according to the model for a thin or thick plate of nanocomposites in air, using effective medium theory (Maxwell-Garnet mixing rule) with appropriate values of the filling factor. This means that in the case of thin samples we have a three-layer structure consisting of:

- medium 1 is air ($\varepsilon_1 = 1$);
- medium 2 is a surface modified ZnS nanoparticles / PMMA nanocomposite of thickness d.
- medium 3 is air ($\varepsilon_3 = 1$);

In the case of a thick film, the second layer is optically thick, so we don't have a third layer. The far-infrared spectra (spectral range of 90–600 cm^{-1}) of pure PMMA thick samples are presented in Fig. 3. The experimental data are presented in circles. Practically, this is a bulk sample, so the standard procedure for calculating the reflection coefficient can be applied (Abstreiter et al. 1984). We used the dielectric function that includes the interaction between the LO phonon and a plasmon, which is described in more detail in ref. (Romcevic et al. 2020):

$$\varepsilon(\omega) = \varepsilon_\infty \frac{\prod_{j=1}^{2}\left(\omega^2 + i\gamma_{lj}\omega - \omega_{lj}^2\right)}{\omega\left(\omega + i\gamma_P\right)\left(\omega^2 + i\gamma_t\omega - \omega_t^2\right)} \prod_{m=1}^{s} \frac{\omega^2 + i\gamma_{LOm} - \omega_{LOm}^2}{\omega^2 + i\gamma_{TOm} - \omega_{TOm}^2} \tag{1}$$

The theoretical spectrum is presented as the solid line in Fig. 3. A phonon was registered around 353 cm^{-1} and two very weak phonons around 360 cm^{-1} and 379 cm^{-1}. Taking into account the results of the Raman spectra (Curcic et al. 2020), it can be concluded that the IR spectrum is much simpler.

In the case of a thick sample of surface modified ZnS nanoparticle / PMMA nanocomposite (Fig. 4), medium 2 was modeled by effective medium theory (Maxwell-Garnet mixing rule) (Maxwell Garnett 1904):

$$\varepsilon_{eff} = \varepsilon_1 + 3f\varepsilon_1 \frac{\varepsilon_2 - \varepsilon_1}{\varepsilon_2 + 2\varepsilon_1 - f\left(\varepsilon_1 - \varepsilon_2\right)} \tag{2}$$

Approximation presented in Eq. (2) describes a homogeneous matrix ε_1 (in this case air with $\varepsilon_1 = 1$) in which spherical nanoparticles with permittivity ε_2 are randomly arranged to occupy a volume fraction *f*. The reflection coefficient, in this case, is given as:

$$R = \left(\sqrt{\epsilon_{eff}} - 1\right) / \left(\sqrt{\epsilon_{eff}} + 1\right)$$

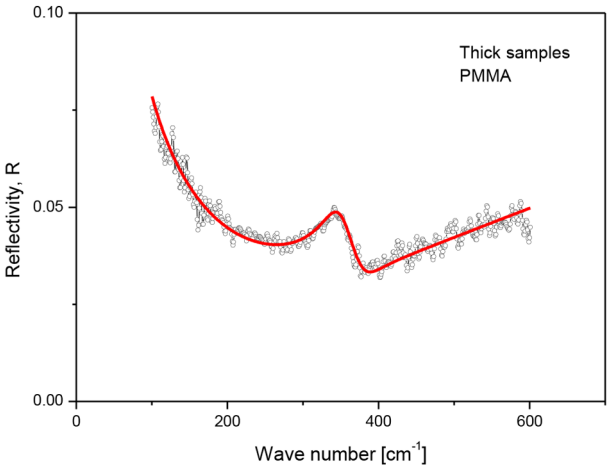

Fig. 3 Far-infrared reflection spectra of thick PMMA (2 mm). The experimentally obtained data points are depicted as circles. The theoretical spectrum is obtained using the model defined by Eq. 1 and the fitting procedure is given as a solid line

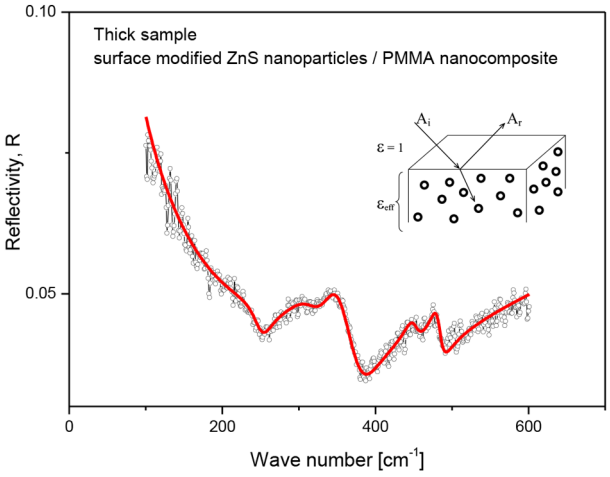

Fig. 4 Far-infrared reflection spectra of thick (2 mm) surface modified ZnS nanoparticles / PMMA nanocomposite. The experimentally obtained data points are depicted as circles. The theoretical spectrum obtained with the model defined by Eq. 2 and the fitting procedure is given as a solid line. Insert a Semantic overview of the sample

The far-infrared spectra of thick surface modified ZnS nanoparticles / PMMA nanocomposite, in the spectral range of 100–600 cm^{-1}, at room temperature are presented in Fig. 4. The experimental data are presented in circles. The sample is thick enough to behave as bulk material which is schematically presented in the inset of Fig. 4. The theoretical spectrum (the solid line in Fig. 4) is obtained by using a dielectric function defined by Eq. 2. The agreement of the theoretical model obtained in this manner with the experimental results is excellent. A filling factor of f=0.02 was obtained, which supports our decision to use the Maxwell-Garnet formula. The addition of surface modified ZnS nanoparticles to the bulk of PMMA in this amount led to the preservation of the PMMA spectrum, as basic, with weakly.

expressed ZnS characteristics. The difference in spectra was observed in the region of around 200 cm^{-1}, in the range of 260–350 $cm^{-1,}$ and the region of 400–550 cm^{-1}. These are expected results since these are all characteristics of ZnS (Trajic et al. 2015; Trajic et al. 2016; Curcic et al. 2020). It is interesting to note that ZnS phonons, characterized as overtones and combinations of phonons, left a significant trace on the spectrum. This is a consequence of the fact that the PMMA spectrum in this part is flat without some specifics, while in the area of TO-LO phonons of ZnS, a basic characteristic of PMMA is also positioned.

The far-infrared spectra of pure thin PMMA, in the spectral range of 80–600 cm^{-1}, at room temperature are presented in Fig. 5. The experimental data are presented in circles. The inset in Fig. 5 shows a schematic model of our sample. Medium 1 is air with dielectric functions ε_1 ($\varepsilon_1=1$). Medium 2 is a layer of thickness d with the dielectric constant ε_2 (given with Eq. 1.). The lower layer is air again. The theoretical spectrum (the solid line in Fig. 5.), was obtained using the procedure described in Eq. 3. as given in (Gilic et al. 2013):

$$R_A = \frac{A_r}{A_i} = \frac{\boldsymbol{r}_{12}e^{-i\boldsymbol{\alpha}} + r_{23}e^{i\boldsymbol{\alpha}}}{e^{-i\boldsymbol{\alpha}} + \boldsymbol{r}_{12}\boldsymbol{r}_{23}e^{i\boldsymbol{\alpha}}} \tag{3}$$

where $r_{ij} = (n_i - n_j)/(n_i + n_j) = \left(\sqrt{\epsilon_i} - \sqrt{\epsilon_j}\right)/\left(\sqrt{\epsilon_i} + \sqrt{\epsilon_j}\right)$, are the Fresnel coefficients, A_i and A_r represent amplitudes of the incident and reflection beams, respectively, n is complex index of refraction, ε is the dielectric constant and $\alpha = 2\pi\omega d(\varepsilon_2)^{1/2}$ is the complex

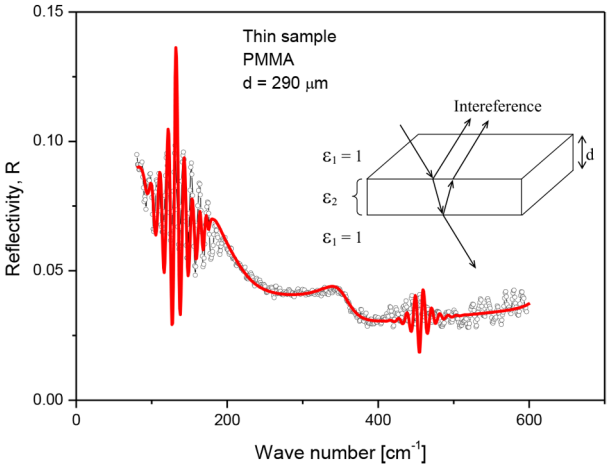

Fig. 5 Far-infrared reflection spectra of thin (290 μm) PMMA. The experimentally obtained data points are depicted as circles. The theoretical spectrum obtained with the model defined by Eq. 3 and fitting procedure is given as solid line. Insert a Schematic overview of the sample

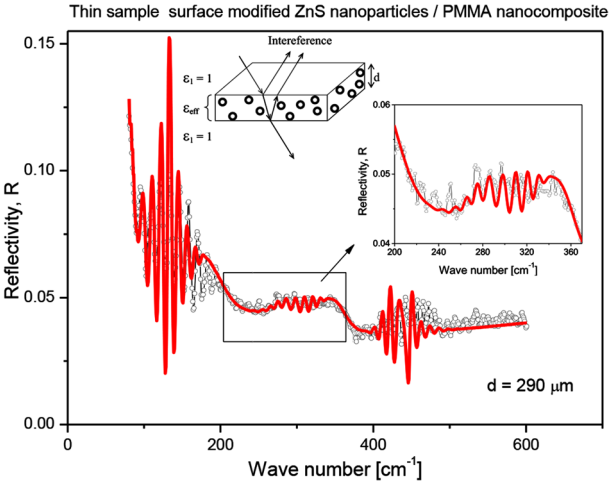

Fig. 6 Far-infrared reflection spectra of thin (290 μm). surface modified ZnS nanoparticles / PMMA nanocomposite. The experimentally obtained data points are depicted as circles. The theoretical spectrum obtained with the model defined by Eq. 3 and fitting procedure is given as solid line. Insert 1: Schematic overview of the sample. Insert 2: Spectrum in the range of ZnS TO-LO phonons

phase change related to the absorption in the crystal layer with the thickness *d*. Reflectance, *R*, is given as: $R = |R_A|^2$.

The combination of the layer thickness d and the PMMA parameters gives interference in two ranges. The first range is intense interference of 100–190 cm^{-1}. For d=290 μm, by a suitable choice of parameters, a good agreement of the theoretical and experimental spectra was obtained, i.e. positions of interference maxima and minima, and thus the periods of these oscillations. In the case of the second range at about 450 cm^{-1}, the theoretical interference is just in a good position. There is a deviation in the intensity of interference in both bands. The agreement of the experimental and theoretical spectra in the rest is good. The theoretical spectrum reproduces the first 9 interference maxima.

The far-infrared spectra of thin surface modified ZnS nanoparticles / PMMA nanocomposite, in the spectral range of 80–600 cm^{-1}, at room temperature are presented in Fig. 6. The experimental data are presented in circles. A schematic representation of the sample is given in inset 1 in Fig. 6. Medium 1 is air with dielectric functions ε_1 (ε_1=1). Medium 2 is

a nanocomposite layer of thickness d and dielectric constant ε_2, described by Eq. 2. In these equations, the parameters describing the spectra from Figs. 3 and 4 are used. The lower layer is again air. The theoretical spectrum (the solid line in Fig. 6) was obtained using the procedure described in Eq. 3. Filling factor f = 0.02 was obtained. All conclusions made by analyzing the spectrum from Fig. 5 can be accepted in this case as well. Additionally, the characteristics of ZnS nanoparticles are visible. However, the main difference in the spectra in Figs. 5 and 6 is in the complementary interference that occurs in the TO-LO phonon range of ZnS. That part of the spectrum is shown in detail in inset 2 in Fig. 6. This interference is of lower intensity than that registered in Fig. 5, but it is clear that it exists. We can easily conclude that it is the result of the existence of surface modified ZnS nanoparticles in PMMA. The problem with the reproduction of the interference intensity remained in this sample as well. The agreement of the experimental and theoretical spectra in the rest is good. The theoretical spectrum reproduces the first 8 interference maxima in the first band and all interference maxima in the TO-LO phonon range of ZnS. It is interesting to note that the distance between the interference maxima is not constant, but varies from about 8 cm^{-1} to 13 cm^{-1} in the case of the PMMA sample, and from 11 cm^{-1} to 14 cm^{-1} in the case of nanocomposites.

To our opinion, the discrepancy between the intensity of interference in the experimental and theoretical spectra is a consequence of the simplicity of our model. Namely, in PMMA samples, with and without added surface modified ZnS nanoparticles, the thickness of the thin film is not equal in all parts of the sample. i.e. the boundary surfaces are not ideally parallel. The occurrence of interference is very sensitive to both parameters. Therefore, the period of oscillation has deviations from the constant. Of course, this can also be correlated with the frequency dependence of the dielectric function.

Regardless of this problem, we believe that research in the field of the influence of the addition of nanoparticles in polymer thin films on the effects of interference should be continued with the aim of application in the measurement technology and sensor industry.

5 Conclusion

Results of the present study showed that the inclusion of surface-modified semiconductor nanoparticles into polymer films induces novel interference effects. Namely, in the case of a PMMA thin sample (about 290 μm) intense, well-defined interference was registered in the range of 90 to 200 cm^{-1}, while significantly weaker and less well-defined interference was registered in the range around 450 cm^{-1}. In the thin surface modified ZnS nanoparticles / poly (methylmethacrylate) - (PMMA) nanocomposites sample, in addition to the interference induced by sample thickness, interference induced by the existence of ZnS nanoparticles (crystallite size at about 2.3 nm) was also observed, located between TO and LO phonons of ZnS. The specific nature of the effect is related to the fact that for the same thin film thickness, we can modify the basic interference effect by designing the properties of nanocomposites. We registered the new effect - modified semiconductor nanoparticles induced interference in thin polymer samples, suitable for use in interferometry.

Author contributions All authors read and approved the final manuscript.

Funding This research was supported by the Science Fund of the Republic of Serbia, Grant No. 7504386, Nano object in own matrix – Self composite – NOOM-SeC.

Data availability Experimental data will be made available on request.

Declarations

Ethical approval Not applicable.

Competing interests The authors have no competing interests to declare that are relevant to the content of this article.

References

Abstreiter, G., Cardona, M., Pinczuk, A.: In: Cardona, M., Guntherodt, G. (eds.) Light Scattering in Solids. IV. Springer-, Berlin (1984). https://doi.org/10.1007/3-540-11942-6

Colvin, V.L., Schlamp, M.C., Alivisatos, A.P.: Light-emitting diodes made from cadmium selenide nanocrystals and a semiconducting polymer. Nature. **370**, 354–357 (1994). https://doi.org/10.1038/370354a0

Curcic, M., Hadzic, B., Gilic, M., Radojevic, V., Bjelajac, A., Radovic, I., Timotijevic, D., Romcevic, M., Trajic, J., Romcevic, N.: Surface optical phonon (SOP) mode in ZnS/PMMA nanocomposites. Phys. E: Low-dimensional Syst. Nanostruct. **115**, 113708, 1–6 (2020). https://doi.org/10.1016/j.physe.2019.113708

Dabbousi, B.O., Bawendi, M.G., Onitsuka, O., Rubner, M.F.: Electroluminescence from CdSe quantum-dot/polymer composites. Appl. Phys. Lett. **66**, 1316–1318 (1995). https://doi.org/10.1063/1.113227

Dutkova, E., Balaz, P., Pourghahramani, P., Velumani, S., Ascencio, J.A., Kostova, N.G.: Properties of Mechanochemically synthesized ZnS nanoparticles. J. Nanosci. Nanotechnol. **9**, 6600–6605 (2009). https://doi.org/10.1166/jnn.2009.1361

Dzenis, Y., Nanocomposites, S.: Science. **319**, 419 (2008). https://doi.org/10.1126/science.1151434

Gilić, M., Trajić, J., Romčević, N., Romčević, M., Timotijević, D.V., Stanišić, G., Yahia, I.S.: Optical properties of CdS thin films. Opt. Mater. **35**, 1112–1117 (2013). https://doi.org/10.1016/j.optmat.2012.12.028

Maxwell Garnett, J.C.: Colours in metal glasses and in metallic films. Phil Trans. R Soc. A. **203**, 385–420 (1904). https://doi.org/10.1098/rspl.1904.0058

Murray, C.B., Norris, D.J., Bawendi, M.G.: Synthesis and characterization of nearly monodisperse CdE (E=S, Se, Te) semiconductor nanocrystallites. J. Am. Chem. Soc. **115**, 8706–8715 (1993). https://doi.org/10.1021/ja00072a025

O'Regan, B., Grätzel, M.: A low-cost, high-efficiency solar cell based on dye-sensitized colloidal TiO2 films. Nature. **353**, 737–740 (1991). https://doi.org/10.1038/353737a0

Peppas, N.A., Langer, R.: New chalenges in biomaterials. Science. **263**, 1715–1720 (1994). https://doi.org/10.1126/science.8134835

Romcevic, N., Hadzic, B., Romcevic, M., Paunovic, N., Sibera, D., Narkiewicz, U., Kuryliszyn-Kudelska, I., Ristic-Djurovic, J.L., Dobrowolski, W.D.: Structural and optical properties of ZnO-Al_2O_3 nanopowders prepared by chemical methods. J. Lumin. **224**, 1–11 (2020). https://doi.org/10.1016/j.jlumin.2020.117273

Romcevic, N., Curcic, M., Radojevic, V., Trajic, J., Paunovic, N., Babic, B., Hadzic, B., Romcevic, M.: Modulated interference effect by ZnS nanoparticles / 3-Mercaptopropyltrimethoxysilane quasi core-shell structure: Far-infrared spectroscopy, Optoelectronics and Advanced materials -. Rapid Commun. **16**(7–8), 359–363 (2022)

Stavenga D.G.: Thin Film and Multilayer Optics cause structural colors of many insects and birds. Mater. Today: Proc. **1**, 109–121 (2014). https://doi.org/10.1016/j.matpr.2014.09.007

Steel, W.H., Interferometry: Cambridge: Cambridge University Press (1986)

Trajic, J., Kostic, R., Romcevic, N., Romcevic, M., Mitric, M., Lazovic, V., Balaz, P., Stojanovic, D.: Raman spectroscopy of ZnS quantum dots. J. Alloy Comp. **637**, 401–406 (2015). https://doi.org/10.1016/j.jallcom.2015.03.027

Trajić, J., Romčević, M., Romčević, N., Babić, B., Matović, B., Balaž, P.: Far-infrared spectra of mesoporous ZnS nanopaticles. Opt. Mater. **57**, 225–230 (2016). https://doi.org/10.1016/j.optmat.2016.05.004

Authors and Affiliations

Nebojsa Romcevic[1] · Branka Hadzic[1] · Milica Curcic[1] · Vesna Radojevic[2] · Novica Paunovic[1] · Maja Romcevic[1]

✉ Branka Hadzic
branka@ipb.ac.rs

Nebojsa Romcevic
romcevi@ipb.ac.rs

Milica Curcic
milicap@ipb.ac.rs

Vesna Radojevic
vesnar@tmf.bg.ac.rs

Novica Paunovic
paun@ipb.ac.rs

Maja Romcevic
romcevic@ipb.ac.rs

[1] Institute of Physics Belgrade, University of Belgrade, Pregrevica 118, Belgrade 11080, Serbia

[2] Faculty of Technology and Metallurgy, University of Belgrade, Karnegijeva 4, Belgrade 11000, Serbia